

Multifunctional CuO nanowire devices: p-type field effect transistors and CO gas sensors

This article has been downloaded from IOPscience. Please scroll down to see the full text article.

2009 Nanotechnology 20 085203

(<http://iopscience.iop.org/0957-4484/20/8/085203>)

The Table of Contents and more related content is available

Download details:

IP Address: 155.69.4.4

The article was downloaded on 03/02/2009 at 14:36

Please note that terms and conditions apply.

Multifunctional CuO nanowire devices: p-type field effect transistors and CO gas sensors

L Liao¹, Z Zhang¹, B Yan¹, Z Zheng¹, Q L Bao², T Wu¹, C M Li², Z X Shen¹, J X Zhang³, H Gong³, J C Li⁴ and T Yu^{1,5}

¹ Division of Physics and Applied Physics, School of Physical and Mathematical Sciences, Nanyang Technological University, 637371, Singapore

² School of Chemical and Biomedical Engineering and Center for Advanced Bionanosystems, Nanyang Technological University, 639798, Singapore

³ Department of Materials Science and Engineering, National University of Singapore, Blk E3A, 7 Engineering Drive 1, 117576, Singapore

⁴ Key Laboratory of Acoustic and Photonic Materials and Devices of Ministry of Educations, Department of Physics, Wuhan University, Wuhan 430072, People's Republic of China

E-mail: Yuting@ntu.edu.sg

Received 10 November 2008, in final form 11 December 2008

Published 2 February 2009

Online at stacks.iop.org/Nano/20/085203

Abstract

We report the properties of a field effect transistor (FET) and a gas sensor based on CuO nanowires. CuO nanowire FETs exhibit p-type behavior. Large-scale p-type CuO nanowire thin-film transistors (10^4 devices in a 25 mm^2 area) are fabricated and we effectively demonstrate their enhanced performance. Furthermore, CuO nanowire exhibits high and fast response to CO gas at 200°C , which makes it a promising candidate for a poisonous gas sensing nanodevice.

(Some figures in this article are in colour only in the electronic version)

1. Introduction

Field effect transistors (FETs) and gas sensors based on semiconductor nanowires (NWs) are important devices in modern technologies [1–4]. A FET is the building block of integrated circuits and the central processing unit of various nanodevices. Up to now, most devices have been based on natural n-type transition metal oxide NWs such as ZnO, In_2O_3 , SnO_2 , etc [1–8]. The synthesis of p-type metal oxide NWs enables novel complementary NW devices and circuits, light-emitting diodes (LEDs), electrically driven nanolasers, multiplexing biosensors, etc, and can open up enormous opportunities for nanoscale electronics, optoelectronics, and medicines [9]. One of the most common ways to produce p-type semiconductor NWs is doping some acceptor impurities into the NWs [3, 4]. However, usually the p-type semiconductor NWs achieved this way present

many obstacles, such as poor stability and reproducibility. Therefore, it is strategically desirable to fabricate and investigate FETs based on p-type metal oxides. Gas sensors play critical roles in many fields such as industrial production, environmental pollution, mining safety, and traffic safety. The sensing mechanisms for n-type semiconductors have been well analyzed and discussed according to the surface depletion and grain boundary models [7, 8]. However, the sensing behavior of one-dimensional p-type materials has not been fully investigated, and the sensing mechanisms are still unclear [10]. Though response is one of the most important aspects for an effective gas sensing device, industrial applications also require good selectivity. Unfortunately, achieving good selectivity of a gas sensor based on metal oxide NW is still a complicated issue and not easy to be resolved.

CuO is an important p-type semiconductor with a band gap of about 1.36 eV [11], which has potential applications in many fields such as high-critical-temperature superconductors [12], photovoltaic materials [13], field emission [14], and catalysis [15].

⁵ Address for correspondence: Division of Physics and Applied Physics, School of Physical and Mathematical Sciences, Nanyang Technological University, 637616, Singapore. URL: www.ntu.edu.sg/home/yuting/

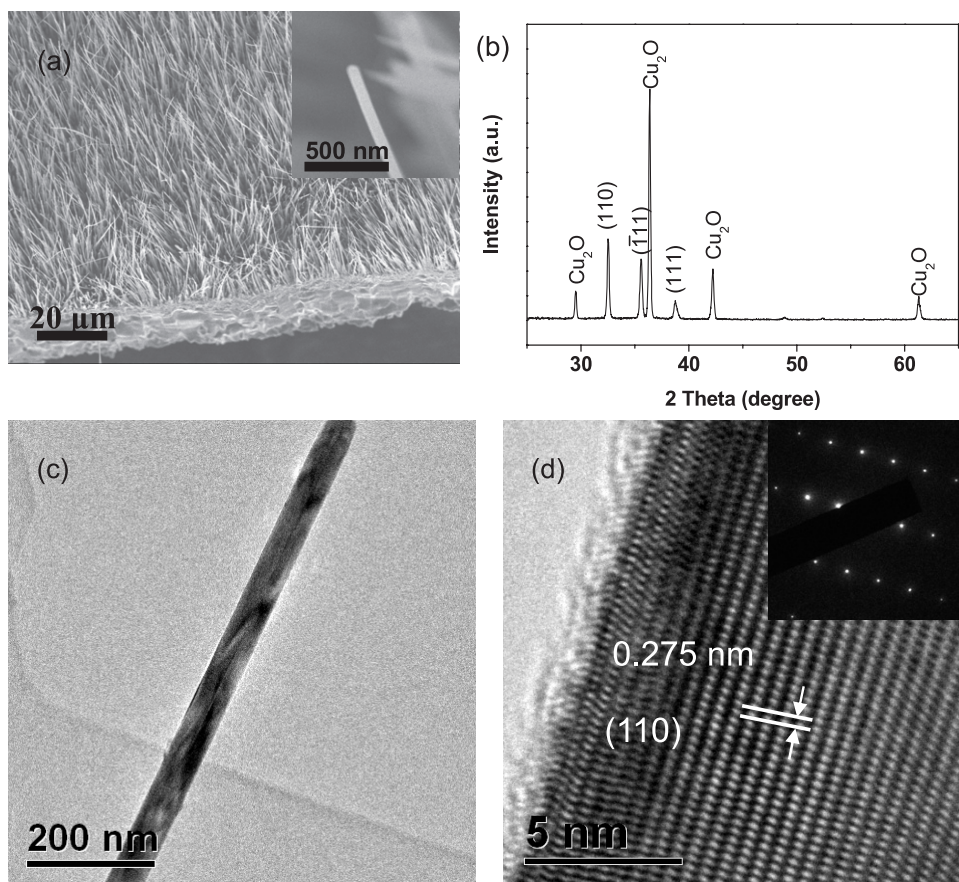


Figure 1. (a) SEM image of CuO NWs on Cu foils; the inset SEM image shows a single CuO NW, (b) XRD pattern of CuO NWs on Cu foil, (c) TEM, and (d) HRTEM images of a single CuO NW. The inset of (d) shows the corresponding SAED pattern.

In this paper, we demonstrate that CuO NW could be a promising candidate for a p-type FET and a gas sensor with good performance. The CuO NW FETs, NW thin-film transistors (TFTs), and gas sensors were fabricated by photolithography. The experimental results indicate that CuO NW is a typical p-type semiconductor. Furthermore, gas sensors made from CuO NWs exhibit high response to CO gas in air at 200 °C.

2. Experimental details

Fresh copper foils (10 mm × 10 mm × 0.1 mm, Aldrich, 99.99%) with a purity of 99.9% (Aldrich) were used as both reagents and substrates for the growth of CuO NWs. The cleaned Cu foil was baked in a box oven under ambient conditions; the heating was fixed at a temperature of 500 °C for 10 h [12]. The as-grown CuO NWs were removed from the substrates by sonication and subsequently dispersed in ethanol. The solution was dropped on SiO₂/Si (i.e. 200 nm insulated SiO₂ film over Si substrate), and then Au contact pads of 100 nm thickness were fabricated by UV lithography and rf sputtering. If the concentration of nanowires was high enough, we always could find a single nanowire between two electrodes. The electrical transport properties were measured with a Suss probe station with a Keithley 4200 SCS

(semiconductor characterization system). Finally, after wire-bonding to a supporting chip, the gas sensing properties of the devices were examined. The testing gases employed in this work were pure air and 5–1200 ppm test gases in air. Different devices were used to measure different gases. The gas response of the devices was defined as the ratio of the electrical resistance in the testing gases (R_g) to that in air (R_a).

3. Results and discussion

The low-magnification scanning electron microscopy (SEM) image given in figure 1(a) shows that the aligned CuO NWs on the substrate are about 20–30 μm in length, and about 50–100 nm in diameter. Figure 1(b) shows the x-ray diffraction (XRD) pattern of the as-grown CuO NWs: both Cu₂O and CuO phases are present, as reported in [16] and [17]. When copper is oxidized in air, the major product is Cu₂O, and CuO is formed slowly only through a second step of oxidation. In this case, the Cu₂O exists as a thin-film precursor for growing CuO NWs during the oxidation treatment of the Cu foil [16]. Our transmission electron microscopy (TEM) results also demonstrate that the nanowires formed in this top layer are crystalline phase CuO. A typical TEM image of the CuO NWs is shown in figure 1(c). Figure 1(d) displays a high-resolution TEM image and a selected area electron diffraction (SAED) pattern of the NW, which shows that the NW is indeed

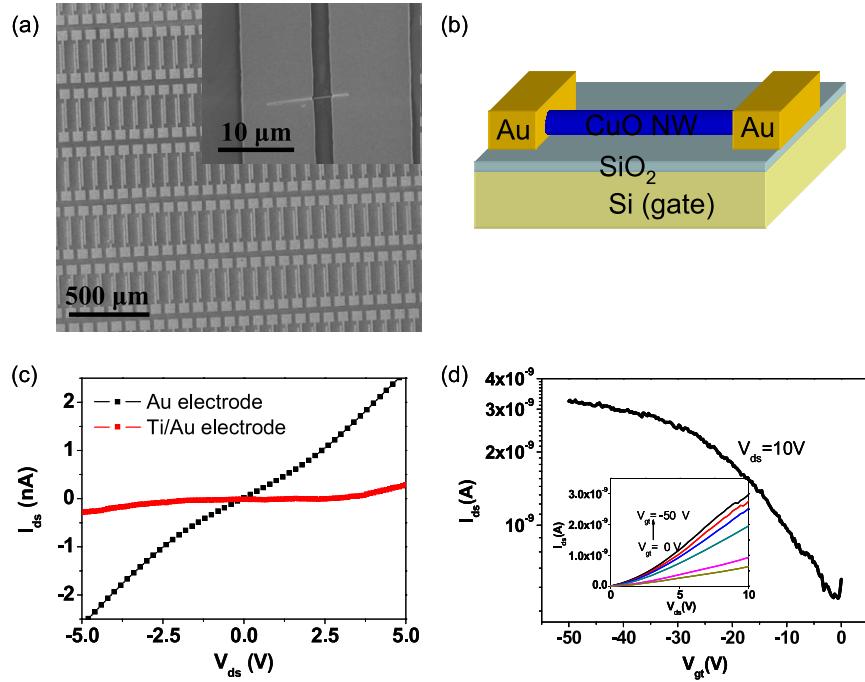


Figure 2. (a) SEM image of many pairs of Au electrode pads; the inset shows a SEM image of a single CuO NW field effect transistor; (b) schematic diagram of the configuration; (c) I - V curves of single CuO NW devices with Ti electrodes and Au electrodes; (d) I_{ds} - V_{gt} curves of a single CuO NW FET; the inset shows I_{ds} - V_{ds} curves of a single CuO NW FET.

single-crystalline CuO. The inter-planar spacing along the NW direction was measured to be 0.275 nm, which corresponds well with the spacing between (110) planes in monoclinic CuO. Besides, the electron diffraction pattern indicates that the growth direction of our CuO NW is along [110].

SEM images of a single CuO NW field effect transistor and many pairs of Au electrode pads are shown in figure 2(a). Figure 2(b) shows the schematic device diagram of a CuO NW field effect transistor. To optimize the performance of the as-fabricated devices, the contact properties were investigated. In our experiment, Ti/Au electrodes were used at first to study the electrical properties of the CuO NW. The corresponding current-voltage (I - V) curves are shown in figure 2(c). Obvious nonlinear characteristics, weak electrical current, and an increment of slopes at high bias voltages were observed, which can be attributed to Schottky barriers at both source and drain contacts. In general, the contact properties depend on the difference of work functions between the electrodes and the semiconducting NWs; the type of majority carriers also affects the contact properties. When the work function of the contact metal is larger than that of the semiconductor, an n-type semiconductor exhibits a Schottky barrier while a p-type semiconductor exhibits ohmic contact [18]. As the work function of Ti (4.3 eV) is smaller than that of CuO (5.2 eV), the observation that Schottky barriers exist between the CuO NW and the Ti contacts implies that the as-grown CuO NW is a p-type semiconductor. To obtain ohmic contact, a high work function metal, Au (5.1 eV), was chosen as the electrodes, instead of Ti. Linear I - V curves were obtained (shown in figure 2(c)), indicating that ohmic contacts were established between Au and CuO.

The inset of figure 2(d) displays the current of drain-source (I_{ds})-the drain-source (V_{ds}) curves of a typical CuO NW FET. From the I_{ds} - V_{ds} curves obtained under gate voltages (V_{gt}) of -50, -40, -30, -20, -10, and 0 V, it can be clearly seen that the conductance of the NW decreases monotonically as the gate potential increases, demonstrating that the CuO NW is a p-type semiconductor. Figure 2(d) shows the I_{ds} - V_{gt} curve of a single NW FET. The field effect mobility (μ) in a typical cylindrical NW with radius r can be expressed as [1, 19]

$$\mu = \frac{dI}{dV_g} \times \frac{\ln(2h/r)}{2\pi\epsilon_0\epsilon_r} \times \frac{L}{V_{ds}} \quad (1)$$

$$g_m = \frac{dI}{dV_g} \quad (2)$$

$$C = \frac{2\pi\epsilon_0\epsilon_r L}{\ln(2h/r)} \quad (3)$$

where V_{gt} is the threshold gate voltage, e is the hole charge, ϵ_r is the relative dielectric constant ($\epsilon_r = 3.9$ for SiO_2), h is the thickness of gate oxide layer, L is the channel length, g_m is the transconductance of the material and C is the nanowire capacitance. $V_{gt} = -2$ V, and the transconductance $g_m = dI/dV_{gt} = 0.24$ nS can be extrapolated from the linear region (-30 to -3 V) of the I_{ds} - V_{gt} curve. The capacitance of the CuO NW is $C = 2.1 \times 10^{-2}$ pF and the mobility is $\mu = 2-5$ $\text{cm}^2 \text{V}^{-1} \text{s}^{-1}$ at $V_g = 0$ V, which is higher than that in previous reports [20, 21].

For comparison with single NW devices, thin-film transistors were fabricated using arrays of parallel CuO NWs. Well-aligned CuO NWs were transferred onto a SiO_2/Si substrate (figure 3(a)) using a physical transfer method [22].

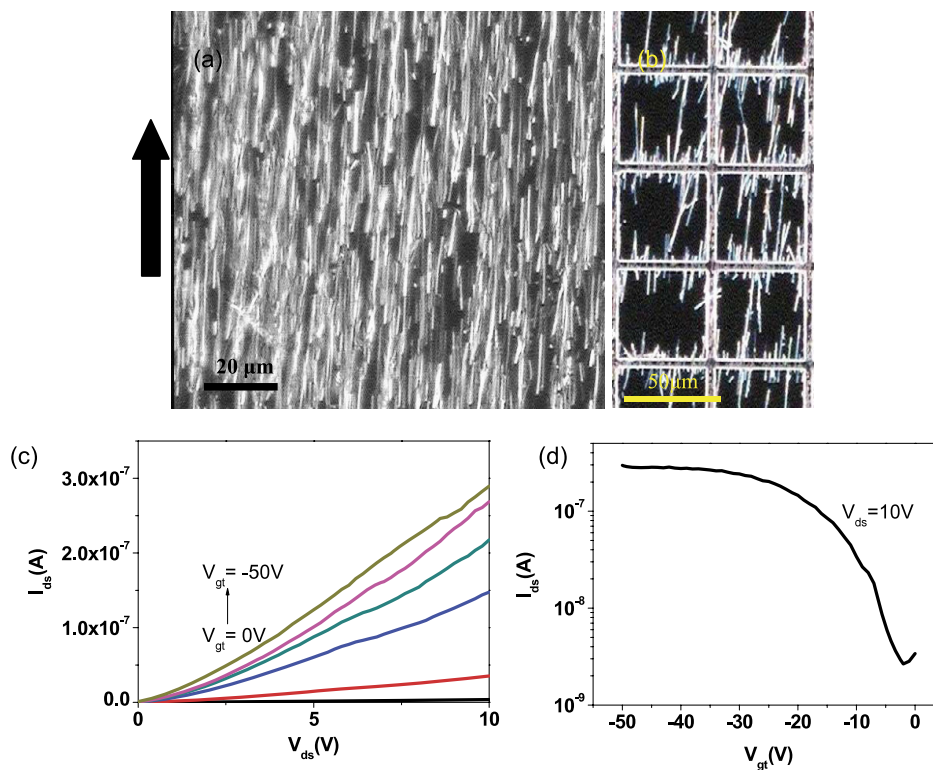


Figure 3. (a) Dark-field optical microscope image of a CuO NW film obtained through the physical transfer method. (b) Optical dark-field microscope image of the TFT device. (c) I_{ds} - V_{ds} curves of the CuO NW-TFT device, (d) I_{ds} - V_{gt} curves of the CuO NW-TFT device.

The overall process involves (i) optimized growth of the CuO NW and (ii) patterned transfer of NWs directly from an NW growth substrate to a device substrate via contact printing. The CuO NWs are oriented on the growth substrate. Then, a patterned device substrate is first firmly attached to a benchtop, and the NW growth substrate is placed upside down on top of the patterned device substrate such that the NWs are in contact with the device substrate. A gentle manual pressure is then applied from the top followed by sliding the growth substrate 1–3 mm. The NWs are well aligned by shear forces during the sliding process. The sliding process results in the direct and dry transfer of NWs from the growth substrate to the desired device substrate chip. Conventional sputter, photolithography, and lift-off processes were used to pattern the device structures. The single-crystalline channel of the NW-based TFT (NW-TFT) devices affords excellent performance metrics. Electrical characterizations obtained on a NW-TFT device with a W/L ratio of 10 (width of channel, $W = 50 \mu\text{m}$, gap of channel, $L = 5 \mu\text{m}$) are shown in figure 3(b). There are about 10^4 units in a 25 mm^2 area. The device displays enhancement-mode p-type transistor behavior, with clear linear regions observed in the I_{ds} - V_{ds} output curves (figure 3(c)). Significantly, from the I_{ds} - V_{gt} shown in figure 3(d), a large on-current $I_{on} = 0.3 \mu\text{A}$, transconductance of $0.2 \mu\text{S}$, mobility of $15 \text{ cm}^2 \text{ V}^{-1} \text{ s}^{-1}$ at $V_g = 0 \text{ V}$, and on/off ratio of 100 were obtained. Compared with the single CuO NW FET, the NW-TFT device shows better performance because there are more conductance channels in a device.

In recent years, many gas sensors based on n-type metal oxide NWs have been reported, such as ZnO, SnO₂ etc [23, 24].

Typically, metal oxide materials are sensitive to reductive gases because of the modulation of the depletion layer [23]. Herein, we fabricated gas sensors based on p-type single CuO NW. Interestingly, we found that they have high response to carbon monoxide. Figure 4(a) shows the gas response against the working temperature of the sensors made of CuO NW. Obviously, the relationship between the gas response and the operating temperature presented a trend of ‘increase–maximum–decay’ to 500 ppm CO. It is thus that we chose 200°C as the operating temperature to study the behavior of both CuO sensors at varied concentrations of CO. Figure 4(b) is the corresponding gas response versus time curve of a single CuO NW gas sensor subjected to CO and ethanol with various densities at 200°C . It can be seen that the CuO NW sensor has a good sensing performance, higher CO response, and shorter response time (less than 10 s). Similar results, which are not shown here, have been obtained for another five gas sensors. The curve of sensitivity versus CO concentration is shown in figure 4(c); the sensitivity of the sample exhibits nonlinear behavior with CO concentration. The sensitivity increases with increase in the CO gas concentration. In our system, the sensor could detect above 5 ppm CO gas in air. When the CO concentration is higher than 1000 ppm, the response does not change obviously. The linear range of the calibration curve is from 50 to 800 ppm. To further probe the selectivity of the CuO NW sensor, we also measured the response of the same sensor to other 500 ppm gases, including H₂, ethanol, NO₂, and H₂S, under a bias voltage of 5 V. The response of the CuO NW sensor to the different gases is shown in figure 4(d). The responses of the CuO sensor to H₂, ethanol, NO₂, and

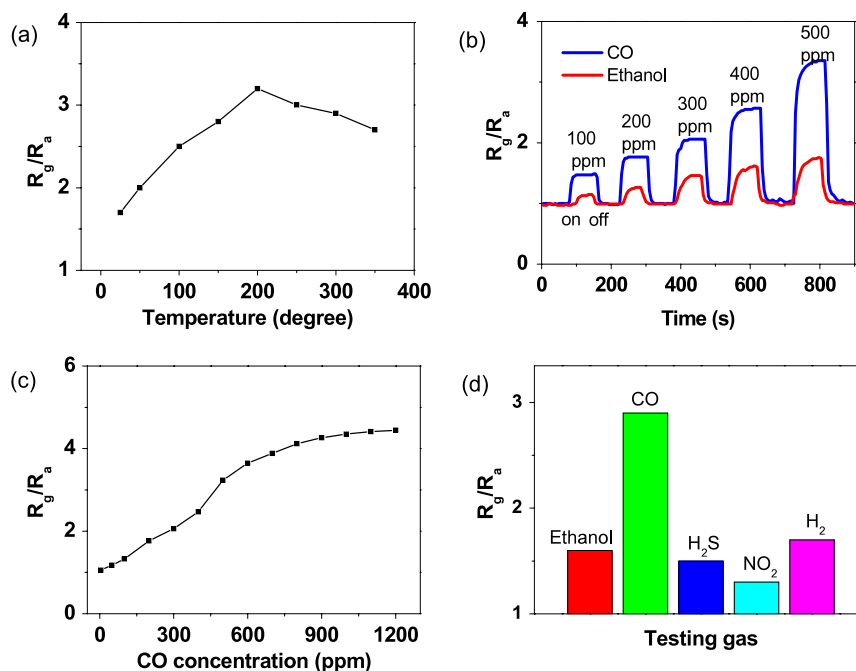


Figure 4. (a) The gas response curves to 500 ppm CO of a CuO NW at different temperatures; (b) the gas response curve of a single CuO NW for CO and ethanol; (c) response versus CO concentration in the range 5–1200 ppm; (d) response of a single CuO NW sensor to different gases with a fixed concentration of 500 ppm.

H₂S are much lower than that to CO. Compared with sensors based on SnO₂ and ZnO, the CuO sensor shows an obvious advantage when a selective detection of CO gas is desired. We also measured the relationship between the response and gate voltage; however, the results is the same as in the previous reports and no new phenomenon was observed [6, 25].

The mechanism of sensing reducing gas by CuO NWs is elucidated as below. When in contact with a reducing gas (electron donator), such as CO, H₂, or ethanol, the negatively charged oxygen (O⁻) adsorbed on the CuO NW surface will react [26]. The reaction between the reducing gas and O⁻ leads to a decrease of the hole density in the surface charge layer and an increase of the CuO resistance. Previous works reported that Cu²⁺ plays a very important role in adsorbing CO molecules in CO sensing [26, 27]. When CO molecules are adsorbed on the surface of the CuO NW, they are preferably adsorbed and form bonds on the Cu²⁺ sites. The Cu–CO bonding consists of the donation of CO 5σ electrons to the metal and the reverse donation of π-electrons from d orbitals of Cu to CO. In this way, the adsorption and reaction at the Cu sites enhance the reaction of CO with the oxygen species and result in the enhancement of the CO reactivity observed in the CuO NW sensor [28].

4. Conclusions

In conclusion, CuO NW can perform as the channel material in p-type FET devices with field effect mobilities over 2–5 cm² V⁻¹ s⁻¹. The NW-TFT devices were found to exhibit better performances than the single CuO NW FET, showing higher on/off ratio and on-current. This study could render

a large-scale manufacturing process for applications of high-performance p-type NW-based thin-film devices. Furthermore, the single CuO NW-based gas sensor shows high and fast response to CO in air. This type of gas sensor is expected to have broad applications in the fast detection of poisonous CO gas in various environments.

Acknowledgment

LL acknowledges support of this work by the Singapore Millennium Foundation 2008 scholarship.

References

- [1] Dattoli E N, Wan Q, Guo W, Chen Y B, Pan X Q and Lu W 2007 *Nano Lett.* **7** 2463
- [2] Wan Q, Dattoli E N, Fung W Y, Guo W, Chen Y B, Pan X Q and Lu W 2006 *Nano Lett.* **6** 2909
- [3] Xiang B, Wang P W, Zhang X Z, Dayeh S A, Aplin D P R, Soci C, Yu D P and Wang D L 2007 *Nano Lett.* **7** 323
- [4] Yuan G D, Zhang W J, Jie J S, Fan X, Zapien J A, Leung Y H, Luo L B, Wang P F, Lee C S and Lee S T 2008 *Nano Lett.* **8** 2591
- [5] Fan Z Y, Wen X G, Yang S H and Lu J G 2005 *Appl. Phys. Lett.* **87** 013113
- [6] Fan Z Y, Wang D W, Pai C C, Tseng W Y and Lu J G 2004 *Appl. Phys. Lett.* **85** 5923
- [7] Liao L, Lu H B, Li J C, Liu C, Fu D J and Liu Y L 2007 *Appl. Phys. Lett.* **91** 173110
- [8] Li C, Zhang D H, Liu X L, Han S, Tang T, Han J and Zhou C W 2003 *Appl. Phys. Lett.* **82** 1613
- [9] Huang Y D, Duan X F and Lieber C M 2005 *Small* **1** 142
- [10] Koffyberg F P and Benko F A 1982 *J. Appl. Phys.* **53** 1173
- [11] Guo X L, Wang G X, Yang J, Park J S and Wexler D 2008 *J. Mater. Chem.* **18** 965
- [12] Eskes H, Tjeng L H and Sawatzky G A 1990 *Phys. Rev. B* **41** 288

- [13] Liu Y L, Liao L, Li J C and Pan C X 2007 *J. Phys. Chem. C* **111** 5050
- [14] Zhu Y W, Yu T, Cheong F C, Xui X J, Lim C T, Tan V B C, Thong J T L and Sow C H 2005 *Nanotechnology* **16** 88
- [15] Avgouropoulos G, Ioannides T, Papadopoulou C, Batista J, Hocevar S and Matralis H K 2002 *Catal. Today* **75** 157
- [16] Yu T, Zhao X, Shen Z X, Wu Y H and Sow C H 2004 *J. Cryst. Growth* **268** 590
- [17] Jiang X C, Herricks T and Xia Y N 2002 *Nano Lett.* **2** 1333
- [18] Sze S M 1981 *Physics of Semiconductor Devices* (New York: Wiley)
- [19] Wunnicke O 2006 *Appl. Phys. Lett.* **89** 083102
- [20] Figueiredo V, Elangovan E, Goncalves G, Barquinha P, Pereira L, Franco N, Alves E, Martins R and Fortunato E 2008 *Appl. Surf. Sci.* **254** 3949
- [21] Wu H, Lin D D and Pan W 2006 *Appl. Phys. Lett.* **89** 133125
- [22] Javey A, Nam S, Friedman R S, Yan H and Lieber C M 2007 *Nano Lett.* **7** 773
- [23] Liao L, Lu H B, Li J C, He H, Wang D F, Fu D J and Liu C 2007 *J. Phys. Chem. C* **111** 1900
- [24] Comini E, Faglia G, Sberveglieri G, Pan Z W and Wang Z L 2002 *Appl. Phys. Lett.* **81** 1869
- [25] Liao L, Zheng Z, Yan B, Zhang J X, Gong H, Li J C, Liu C, Shen Z X and Yu T 2008 *J. Phys. Chem. C* **112** 10784
- [26] Zhang G and Liu M 2000 *Sensors Actuators B* **69** 144
- [27] Gong H, Hu J Q, Wang J H, Ong C H and Zhu F R 2006 *Sensors Actuators B* **115** 247
- [28] Chen H Y, Lau S P, Chen L, Lin J, Huan C H A, Tan L K and Pan S J 1999 *Appl. Surf. Sci.* **152** 193